2052

LA-UR-80-1159

TITLE: DEEP PENETRATION CALCULATIONS

AUTHOR(S): William L. Thompson
O.L. Deutsch
T.E. Booth

SUBMITTED TO: Proceedings of Seminar on Theory and Applications of Monte Carlo Methods



University of California

LOS ALAMOS SCIENTIFIC LABORATORY
Post Office Box 1663 Los Alamos, New Mexico 87545
An Affirmative Action / Equal Opportunity Employer

# DEEP-PENETRATION CALCULATIONS

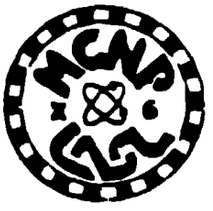

W. L. Thompson
O. L. Deutsch
T. E. Booth
Group X-6
Monte Carlo, Applications and Transport Data Group
Theoretical Applications Division
Los Alamos Scientific Laboratory
Los Alamos, New Mexico 87545

## ABSTRACT

Several Monte Carlo techniques are compared in the transport of neutrons of different source energies through two different deep-penetration problems each with two parts. The first problem involves transmission through a 200-cm concrete slab. The second problem is a 90° bent pipe jacketed by concrete. In one case the pipe is void, and in the other it is filled with liquid sodium.

Calculations are made with two different Los Alamos Monte Carlo codes: the continuous-energy code MCNP and the multigroup code MCMG. With MCNP, seve al techniques and combinations are evaluated: analog Monte Carlo, geometry splitting with Russian roulette, the exponential transformation, a weight window (constraining the upper and lower particle weights to be within certain limits), and using a combination of random walk/deterministic schemes. With MCMG, a comparison is made between continuous-energy and multigroup Monte Carlo and also between different multigroup scattering models (including the one used by the MORSE code).

Several unexpected results were found in the comparisons of the various calculations. For example, compared to continuous-energy calculations, multigroup calculations with standard cross-section weighting (for both Monte Carlo and $S_n$) underpredict the neutron leakage transmitted through the 200-cm concrete slab by a factor of four.

When considering different techniques for reducing the product of variance and computing time with regard to ease of use, reliability, and effectiveness, we find geometric splitting with Russian roulette to be a superior technique. The weight window, however, appears to be more effective than originally anticipated.

## INTRODUCTION

Several Monte Carlo techniques are compared in the transport of neutrons of different source energies in two different deep-penetration problems. The first problem involves transmission through a 200-cm-thick concrete slab. The second problem is a 90° bent pipe jacketed by concrete. In one case the pipe is filled with liquid sodium, and in another case it is void.

In actual shielding applications, one might need to account for photon production and transport, streaming paths, the exact compositions of the shielding material including rebar, and other factors depending on the problem. For example, for 14-MeV neutrons incident on 200 cm of concrete, Oak Ridge concrete reduces the transmitted dose by a factor of ten better than does Los Alamos concrete. All the above considerations, however, are beyond the scope of this paper.

Rather than addressing particular and detailed shielding problems, the purpose of this paper is to apply different Monte Carlo techniques to problems of general interest to the shielding community and to compare the merits of the techniques. The problems considered here have nontrivial attenuations, and an attempt has been made to select representative features of real shielding problems without incorporating arbitrary or extraneous detail. In addition to a comparison of methods, results such as leakage, flux, and dose rate are presented, and we believe these results to be reliable. Doses throughout this paper refer to biological dose and were obtained with the ANSI[1] flux-to-dose conversion factors. By providing these benchmark-type results, others may wish to compare results from the same problems using different calculational tools. Interesting comparisons could be then made in terms of accuracy and efficiency between MCNP and other Monte Carlo codes (such as MORSE, TRIPOLI, or SAM-CE) and other calculational techniques such as $S_n$ or hand calculations using buildup factors.

Basically, several techniques such as the exponential transformation and geometrical splitting with Russian roulette will be compared using the continuous-energy code MCNP[2] with virtually no approximations, MCNP with a pseudo-multigroup set of cross sections, and a true multigroup version of MCNP called MCMG.[3] All calculations done with MCMG are with 30 neutron energy groups. MCMG has the option to represent the distribution of scattering angles for group-to-group transfers by equiprobable cosine bins or by MORSE-type discrete scattering angles.[4] The pseudo-multigroup cross-section set in which the reaction cross sections have been collapsed into 240 energy groups for use with MCNP is referred to as the discrete-reaction data (DRXS). More details can be obtained about MCNP and MCMG in another paper by Thompson and Cashwell given at this seminar.

The amount of computer memory required for cross-section data for the ten constituents of ordinary Portland concrete is given in Table 1 as a function of calculational method, data set, and energy range.

About six hours of CDC-7600 computer time were used for the calculations reported in this paper. The multigroup calculations were done by Deutsch, Booth did the calculations with the exponential transformation and the weight window, and the rest of the calculations were done by Thompson.

Table 1. Neutron Cross-Section Storage for Portland Concrete

| Mode | $Words_{10}$ |
|---|---|
| MCNP, ENDF/B-V<br>20 MeV < E < 0.00912 MeV | 297462 |
| MCNP, ENDF/B-IV<br>20 MeV < E < 0.00912 MeV | 133091 |
| MCNP, DRXS (ENDF/B-IV)<br>20 MeV < E < 0.00912 MeV | 42952 |
| MCMG, 30 group<br>20 MeV < E < $10^{-4}$ eV | 23000 |
| MCNP, ENDF/B-V<br>20 MeV < E < $10^{-5}$ eV | 310621 |
| MCNP, ENDF/B-IV<br>20 MeV < E < $10^{-5}$ eV | 139316 |
| MCNP, DRXS (ENDF/B-IV)<br>20 MeV < E < $10^{-5}$ eV | 45852 |
| MCNP, ENDF/B-V<br>104 keV < E < 8.32 eV | 56161 |

All calculations for this paper were done with ordinary Portland concrete as found in Schaeffer's book.[5] One calculation (the pencil-beam fission spectrum incident on a 100-cm-radius, 200-cm-thick concrete disk) was also done with the 04 concrete from the ANSI standard.[6] The compositions of these two concretes are listed in Table 2. The transmitted dose through the 04 concrete is 4.7 times higher than through the ordinary Portland concrete, while the transmitted leakage and flux are each about 5.2 times higher (these results are within 5%). All following reported results will be with ordinary Portland concrete.

Table 2. Concrete Compositions

| Element | 04 Wt.% | Portland Wt.% |
|---|---|---|
| H | 0.56 | 1.00 |
| O | 49.81 | 52.9 |
| Si | 31.51 | 33.7 |
| Ca | 8.29 | 4.4 |
| C | -- | 0.1 |
| Na | 1.71 | 1.6 |
| Mg | 0.26 | 0.2 |
| Al | 4.57 | 3.4 |
| S | 0.13 | -- |
| K | 1.92 | 1.3 |
| Fe | 1.24 | 1.4 |
| | ρ=2.339 g/cc | ρ=2.30 g/cc |

All continuous-energy calculations were done with ENDF/B-V cross sections. However, the first problem that will be discussed, the pencil-beam fission spectrum incident on 100-cm-radius by 200-cm-thick concrete, wasalso done with ENDF/B-IV cross sections. There were no perceivable differences in any of the results. The Monte Carlo multigroup calculations were done with ENDF-IV cross sections. If calculations had been made involving heating or photon production, this conclusion of equality between IV and V may not have been true. Again, it is not the purpose of this paper to compare cross sections; this has been extensively done at Los Alamos[7,8] and elsewhere by others.

With regard to the use of different Monte Carlo techniques on a variety of applications, there are no universally valid prescriptions. The only truly effective rule of thumb is to always make two or three short, experimental runs (say of half a minute each) to help discover the characteristics of the particular problem and the effect of varying a parameter or two in a particular variance-reduction technique. There is no substitute for practical experience to guide the approach to a particular problem. What works in one situation in no way guarantees success in another situation and may even be harmful. A good Monte Carlo code should provide a variety of standard summary and diagnostic information to help understand what is happening in a given problem. In doing the calculations for this paper, we encountered some surprises to our intuition. However, short, preliminary runs provided the necessary insight for the final runs.

Finally, before getting down to business, comparisons between the various techniques will be done on the basis of a relative figure of merit, FOM = $1/(\sigma^2 t)$ where $\sigma$ is the standard error associated with a result of the

calculation and t is the computer time required. For example, if it took 30 minutes to get a 4% error, 20.8 is the figure of merit. Note that to compare your FOM to the ones reported in this paper, you will also need to factor in the speed of your computer system relative to ours. All calculations reported by us were done on a CDC-7600 computer. All reported errors represent one standard deviation. Note that there is also an error associated with the figure of merit, a variance of the variance. In the following calculations, we attach no significance to small differences in the FOM such as between 62 and 55.

The factor $\sigma^2 t$ is directly related to the dollar cost of running a job. It is important to note that the cost depends both on $\sigma^2$ and t; for example, you may reduce $\sigma^2$ but only at a greater expense in t or vice versa; the product of the two must be reduced to be beneficial. Not explicit in this relation for the total cost of a job is the cost in human time to set a job up and the cost of the preliminary experimental runs to set the parameters. If you spend three days with an elaborate setup and five hours of computer time refining and optimizing the parameters in the best possible way so that your job runs in 10 minutes rather than 20, you have lost. In all the following calculations, we usually made two or three preliminary runs for about a half minute each. We make no claim that our setups and figures of merit are the best, but they are acceptable as being cost-effective. Undoubtedly, someone can make improvements but probably not without diminishing returns.

## VARIANCE-REDUCTION TECHNIQUES

The successful application of the Monte Carlo method to any deep-penetration problem generally requires the use of one or more variance-reduction techniques. In general, one can expect that some techniques or combinations of techniques will be more effective than others in terms of range of applicability, ease of use, reliability, and performance. We measure performance in terms of the figure of merit $1/(\sigma^2 t)$. By reliability, we refer to the possibility of injudicious selection of the parameters of a technique resulting in erroneous answers because an important part of phase space may not have been sampled adequately, if at all. Finally, ease of use refers to the degree of difficulty in determining the parameters of a technique and to the sensitivity of performance to precise selection of the optimal parameters.

Based on many years of experience and observations of users at Los Alamos, the most frequently-used techniques at Los Alamos are geometry splitting with Russian roulette, directional source biasing, survival biasing, and a weight-cutoff game incorporating Russian roulette. These techniques are frequently used in combination. It is assumed that if energy and/or time cutoffs are appropriate for a problem, then they have been used also. The exponential transformation is infrequently used, and in fact, we have discouraged its use. We note all too frequently that the less experience a user has, the more any of the variance reduction

techniques are abused by using the techniques inappropriately, or with several techniques in conjunctionleading to conflicts, or most commonly by biasing too heavily. Any of these problems can result in a wrong answer. It cannot be overemphasized that any variance-reduction technique must be used with caution and understanding.

In the following calculations, several different techniques are tried and compared. For all problems, we compare geometry splitting with Russian roulette, the exponential transformation, a weight window, and DXTRAN. The effect of running the problems in a purely analog fashion will also be illustrated. Other techniques will also be tried but not for all cases. A short description will be given for the main techniques used in these calculations.

A more detailed description can be found in Ref. 2.

## Geometry Splitting with Russian Roulette

MCNP does not split particle tracks upon collision but as a function of spatial location. The geometry is subdivided into several cells, and each cell is assigned an importance. When a track of weight W passes from a cell of importance I to a cell of higher importance I', the track is split into I'/I tracks, each of weight WI/I'. (Non-integer splitting is allowed, but we will consider only integral importance ratios for simplicity.) If a track passes from a cell of importance I' to a cell of lower importance I, Russian roulette is played; a track survives with frequency I/I' and is assigned a new weight of WI'/I if it survives. Generally, the source cell has importance of unity, and the importances increase in the direction of the tally. The importances are chosen to keep the track population roughly constant between the source and the tally.

## Weight Cutoff with Russian Roulette

The weight cutoff is made relative to the ratio of the importance of the source cell to the importance of the cell where weight-cutoff is about to take place. This keeps the geometry-splitting and weight-cutoff games from interfering. If a track's weight falls below quantity WC2 (usually from survival biasing), Russian roulette is played. A track survives with frequency WC2/WC1 and is assigned the weight WC1 if it survives. WC1 and WC2 are generally chosen to be 0.5 and 0.25, respectively, for a starting weight of unity but are problem-dependent.

## Exponential Transformation

This technique allows a track to move in a preferred direction by artificially reducing the macroscopic total cross section in the preferred direction and increasing the cross section in the opposite direction according to

$$\Sigma_{ex} = \Sigma_t(1 - p\mu) \quad , \tag{1}$$

where

$\Sigma_{ex}$ = transformed total cross section,
$\Sigma_t$ = true total cross section,
$p$ = parameter used to very degree, of biasing, $0 \leq p < 1$, and
$\mu$ = cosine of angle between preferred direction and track's velocity.

Upon collision, the track weight is multiplied by

$$w_c = \frac{e^{-p\Sigma_t \mu s}}{1 - p\mu} ,$$

where s is the distance to collision. Note this can lead to a dispersion of weight, and that it is possible for some weights to become very large if the tracks are traveling opposite to the preferred direction.

We have found the exponential transformation by itself to be of limited use. The dispersion of weights that it creates can result in an unreliable sample mean while the sample variance may erroneously indicate an acceptable precision. Furthermore, it is not clear how to choose the biasing parameter p, but we note that it is generally chosen too high - especially by novice users. For the calculations of this paper, the parameter was selected by observing the sample variance as a function of the parameter on a few short runs.

When combined with a weight window to place a bound on the upper and lower weights of tracks, we have found that the exponential transformation can be useful. However, choosing parameters for the weight window can further complicate the problem setup, especially for the inexperienced user.

## Weight Window

A weight window consists of an upper and a lower bound for a particle's weight. If the track weight is less than the lower weight bound, Russian roulette is played and the weight is increased to lie inside the window or the track is killed. If the track weight is above the upper bound then the track is split so that the resulting tracks have their weights within the window. The bounds of the window can be set as a function of energy and spatial position.

This weight-window capability is presently not a permanent feature of MCNP. It is available as a modification and is under evaluation by Group X-6. Among other things, we are trying to learn how to use it. It appears that this technique has merit not only when used with the exponential transformation but in conjunction with other techniques. The bane of any variance-reduction technique is creating a dispersion of weights and especially creating a few tracks with very large weights. The weight window appears to reduce these problems effectively.

## DXTRAN

In a geometry region which is difficult to sample adequately, the DXTRAN scheme of MCNP can be of value. At each collision, contributions of scattered particles are deterministically transported to a spherical neighborhood of interest. These contributions, or pseudo-particles, are placed on a sphere surrounding the neighborhood of interest and then transported in the ordinary random-walk manner. The parent particle giving rise to the pseudo-particle at a collision continues its random walk, but it is killed if it tries to enter the neighborhood during its random walk.

There are actually two DXTRAN spheres. The pseudo-particles are placed on an outer sphere. An inner sphere concentric to the outer one is used to bias the placement of pseudo-particles within the cone defined by the inner sphere and the point of collision.

DXTRAN has certain features in common with a point detector. It also has the disadvantages of a detector: it can significantly increase computation time, and it is susceptible to large-weighted contributions. For these and other reasons, success is not guaranteed when using DXTRAN, and it (like a detector) should be used selectively and carefully.

A useful feature of MCNP is the DD input card. This provides diagnostics pertaining to DXTRAN or point detectors such as the accumulative fraction of the number of contributions, the fractional contribution, and the accumulative fraction of the total contribution - all as a function of mean free path away from the DXTRAN sphere or detector. Having this information from a short run, Russian roulette can be played on contributions a selected number of mean free paths away. This can save substantial computer time.

## Angle Biasing

Angle biasing for the problems of this paper was not applied for two reasons: (1) our experience with angle-biasing techniques is both limited and discouraging, and (2) angle biasing is not a standard MCNP option. We have experience with sampling two different (fictitious) exit densities, namely

$$p_1(\Omega) = \frac{1 + bv}{4\pi} \quad = \text{probability of sampling a unit solid angle about } u,v,w \quad |b| < 1 \tag{3}$$

and

$$p_2(\Omega) = \frac{be^{bv}}{e^{b} - e^{-b}} \frac{1}{2\pi} \quad = \text{probability of sampling a unit solid angle about } u,v,w \quad b > 0. \tag{4}$$

Both of these schemes seem to introduce a large variation in particle weights which is reflected in a poor variance of the sample mean. Use of weight window improves the variance, but only to the point where the variance matches that of the weight window alone.

It is entirely possible that other angle-biasing schemes may perform much better. In particular, angle-biasing schemes in discrete-angle Monte Carlo codes (such as TRIPOLI) can be easily fabricated to avoid large variations in particle weights. This does not appear to be the case in continuous-angle Monte Carlo codes (such as MCNP).

## CONCRETE-SLAB PROBLEMS

A major advantage of Monte Carlo is the ability to calculate with no compromise in geometrical reality. Since the purpose of this paper is to illustrate some variance-reduction techniques, this advantage plays no role in this particular problem. $S_n$ is more appropriate for this problem - but at the possible expense of getting the wrong answer because of the multigroup approximation (as will be seen later in this paper).

This problem consists of two parts. Both parts consist of a 200-cm-long homogeneous cylinder of ordinary Portland concrete with a pencil-beam source of fission-spectrum neutrons incident along the axis. In one case the radius of the cylinder is 100 cm, and in the other the radius of the cylinder is 20 cm. The object is to tally the net neutron leakage (or current) across the face opposite the source for comparison of all the methods. However, the transmitted flux and biological dose were also calculated by MCNP. The geometry of both cases is illustrated in Fig. 1.

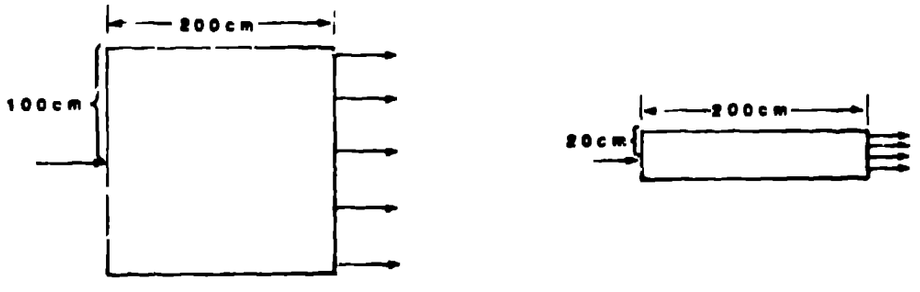


Figure 1. Concrete Slab Problems.

The source energy spectrum is defined according to the Maxwellian representation of the fission spectrum:

$$f(E) = \frac{2}{\sqrt{\pi}T}\sqrt{\frac{E}{T}}\, e^{-E/T} \quad , \tag{5}$$

where we have chosen the parameter T = 1.30 MeV that produces an average source energy of 1.95 MeV. A prescription that was used to sample from

this spectrum for MCNP is in the Appendix. For the multigroup calculations with MCMG, the spectrum was analytically integrated to determine the group sources:

$$\int_{E_{g+1}}^{E_g} f(E)\,dE = \frac{2}{\sqrt{\pi}}\left[\sqrt{\frac{E_{g+1}}{T}}\,e^{-E_{g+1}/T} - \sqrt{\frac{E_g}{T}}\,e^{-E_g/T}\right] + \left[\operatorname{erf}\left(\sqrt{\frac{E_g}{T}}\right) - \operatorname{erf}\left(\sqrt{\frac{E_{g+1}}{T}}\right)\right] \quad . \tag{6}$$

The group sources are listed in the Appendix.

A short adjoint run with MCMG plus an $S_n$ calculation indicated that source particles below 3.68 MeV (this corresponds to one of the multigroup boundaries) made few tally contributions. More precisely, about 10% of the transmitted leakage results from source neutrons below 3.68 MeV. Therefore, the source spectrum was sampled for energies only above 3.68 MeV. These high-energy-source particles account for 12.929% of the total source particles in the unaltered spectrum. Therefore, all results were multiplied by 0.12929 to normalize to one total source neutron. By biasing the source in this manner, the figure of merit for MCNP calculations increased by a factor of two.

For the 3.68-MeV truncated fission spectrum, 200 cm of concrete is about 25 mean free paths thick; for the full, unaltered spectrum, the 200-cm-slab is about 28 mean free paths. In the first 10 cm, the average mean free path is about 6 cm. After only a few more centimeters into the concrete though, the average mean free path becomes about 4.5 cm and remains very close to this throughout the 200-cm thickness. The energy cutoff for the calculations was set at 0.00912 MeV (again this corresponds to one of the group boundaries) because only a couple of percent of the transmitted neutron dose comes from transmitted neutrons with an energy less than this. Using this cutoff increases the figure of merit by a factor of about three. There are 18 groups in the multigroup data above 0.00912 MeV. Furthermore, this energy cutoff requires a smaller computer-memory requirement.

To illustrate the effect of the above energy cutoffs and photon production and that the simplification for this academic paper may not be valid for actual shielding problems, MCNP was used for a 10-minute calculation with none of the above cutoffs and also accounted for photon production for a 100-cm radius by only a 100-cm-thick concrete slab. The figure of merit for the total neutron dose is 8.6 using splitting, and the total neutron dose is $8.1 \times 10^{-13} \pm 8.5\%$ mrem/source neutron. The dose from transmitted neutrons above 0.01 MeV is $7.5 \times 10^{-13}$, and the total photon dose is $1.7 \times 10^{-13} \pm 8.5\%$ mrem per source neutron. About 49% of the photons were started in the energy range 2-5 MeV, 2.7 MeV of photon energy were started on the average per neutron, and the average weight of photons started was 0.87 per neutron. Another run was made but with the neutron energy cutoff at 0.01 MeV. The figure of merit increased to about 56, the total neutron dose became $7.2 \times 10^{-13} \pm 6\%$, and the photon dose dropped to $2.6 \times 10^{-15} \pm 18\%$. Now about 14% of the photons start between 2 and 5 MeV,

0.24 MeV of photon energy were started per neutron, and the average weight of photons started was 0.14 per neutron. For 14-MeV neutrons incident on 100 cm of concrete and using no cutoffs or approximations, about 8% of the total dose comes from photons.

## 100-cm-Radius Problem

With the pencil-beam source, the axially penetrating leakage is $8.2 \times 10^{-9} \pm 4.4\%$, the transverse leakage is $1.9 \times 10^{-5}$, and the backscatter leakage is about 35%. Because of the negligible transverse leakage, the problem geometry is equivalent to a homogeneous, semi-infinite slab. About 9.5% of the neutron weight is lost to capture.

In a purely analog case (no splitting, survival biasing, or anything else), except for source energies greater than 3.68 MeV, 21484 source neutrons were started in two minutes of computer time. At 50 cm there were 5409 (25%) neutrons, 83 were at 100 cm, and none were at 150 cm. This is a very clear example of why variance-reduction techniques are necessary.

Adding survival biasing and weight cutoff with WC1 = 0.5 and WC2 = 0.25 to the above example, a slight improvement is noticed in the same two minutes of time: 19336 source particles were reduced to 5477 (28%) at 50 cm, to 102 at 100 cm, and to none at 150 cm. Only three tracks were lost to the Russian roulette part of the weight cutoff game. With WC1 and WC2 increased to 1.0 and 0.5 respectively, 19432 source particles were reduced to 5461 (28%) at 50 cm, to 106 at 100 cm, and to none at 180 cm. Only 121 tracks were lost to Russian roulette. In this problem survival biasing and weight cutoff help a little but not a significant amount. It is a generally accepted practice, however, to use these two techniques routinely (naturally there are exceptions).

To add geometry splitting with Russian roulette, the concrete cylinder was subdivided axially into cells 10-cm-thick by adding plane splitting surfaces; 10 cm was chosen because it is a convenient number and because it allows a couple of mean free paths between splitting surfaces (based on an average of 4.5 cm for a mean free path averaged over collisions). Cell thicknesses of 15 cm worked equally well. The problem was run for half a minute with the importances of all cells set to unity. Part of the standard summary output of MCNP is the track population in each cell, and wherever the population dropped by a factor of two, the importance of that cell was doubled relative to the adjacent cell in the direction of the source. In some places the two-for-one splitting was not enough, so four-for-one splitting was occasionally used. If an incremental cell thickness less than 10 cm had been chosen, two-for-one splitting could have been used throughout. Conversely, greater than 10-cm increments would have led to a more consistent use of four-for-one splitting. A goal is to try to keep the population roughly constant, say within 50%.

For this particular problem, there appears to be little difference in computer efficiency between two-for-one and four-for-one splitting. Other ratios can also be used as necessary. Two-for-one splitting makes it

easier to level the population, but it requires the user to add more cells and surfaces to the problem setup. Four-for-one splitting requires less input from the user and less arithmetic for the computer, but it is harder to level out the population. Going beyond four-for-one splitting introduces greater risk because that implies a fairly large reduction in the population before it is built back up. The danger is that once a sample population deteriorates to a small size, source information associated with the sample can be lost. Once information is lost, it can never be regained. For example, in the analog problem mentioned earlier, at 170 cm we could have introduced the first splitting surface and split 21484-for-one. The track population would be back to its original size, but then the true energy spectrum would be represented by one discrete energy. The old saying about squeezing blood out of a turnip is very appropriate here.

Three iterations of half a minute each were used to set the importances. The ratio of importances between cells, the actual importance assigned to a cell, and the track population in each cell are shown in Table 3 for 91440 source neutrons. In this final run, weight cutoff was played with WC1 = 0.5 and WC2 = 0.25 (both times the starting weight of the neutrons), resulting in 4233 tracks lost to Russian roulette. In the splitting game, 1118990 tracks were created, but 460729 were lost to Russian roulette. Note that in cell 18 the population is too high.

Table 3. Splitting in the 100-cm-Radius by 200-cm-Thick Concrete Problem

| Cell | Importance Ratio | Importance | Track Population |
|---|---|---|---|
| (Source) 1 | 1 | 1 | 94215 |
| 2 | 1 | 1 | 69498 |
| 3 | 2 | 2 | 86168 |
| 4 | 2 | 4 | 86972 |
| 5 | 2 | 8 | 82441 |
| 6 | 2 | 16 | 78332 |
| 7 | 4 | 64 | 140593 |
| 8 | 2 | 128 | 118175 |
| 9 | 2 | 256 | 101254 |
| 10 | 2 | 512 | 86628 |
| 11 | 2 | 1024 | 75750 |
| 12 | 4 | 4096 | 127292 |
| 13 | 2 | 8192 | 102290 |
| 14 | 2 | 16384 | 89315 |
| 15 | 4 | 65536 | 151848 |
| 16 | 2 | 131072 | 123118 |
| 17 | 2 | 262144 | 107322 |
| 18 | 4 | 1048576 | 180848 |
| 19 | 2 | 2097152 | 142741 |
| (Tally) 20 | 2 | 4194304 | 109576 |

For this problem the transmitted leakage is $8.21 \times 10^{-9} \pm 4.4\%$ for neutron leakage, the transmitted dose is $1.22 \times 10^{-17} \pm 4.5\%$ mrem per source neutron, the transmitted flux is $4.10 \times 10^{-13} \pm 4.3\%$ neutrons/cm$^2$, the leakage escaping through the curved cylindrical surface is $1.91 \times 10^{-5} \pm 16\%$ neutrons, the backscattered leakage is $4.51 \times 10^{-2} \pm 0.4\%$, and 6.7 is the figure of merit.

Other splitting games can also be played. The most obvious is a combination of axial and radial splitting. With radial splitting, one could set up a cone as a splitting surface with its vertex at the source point and then intersecting the edge of the exit face. Secondly, rather than a cone, a concentric cylinder could be used with its radius half that of the outer cylinder. It turns out that neither of these approaches results in much (if any) gain in this problem. What small amount is gained in reducing $\sigma^2$ is lost by an increase in t because of the added arithmetic for the computer.

There is a frequently-heard rule of thumb for geometry splitting that says split two-for-one every mean free path, but you do not hear if this means a mean free path based on source energy or average energy of the particles in the geometry. In this problem, a mean free path based on a source energy is about 8 cm and about 4.5 cm averaged over collisions. Splitting two-for-one every 4.5 cm in only a 100-cm-thick slab of concrete, 1 source neutron had been split into a population of 440 at 50 cm and 12740 at 100 cm and required 0.96 minutes of computer time. Splitting two-for-one every 8 cm in a similar 100-cm-thick slab of concrete was better; 335 source neutrons required 0.52 minutes of computer time and were split into a population of 1597 at 50 cm and 1904 at 75 cm. Obviously, this rule of thumb applied by either method leads to oversplitting.

Using the weight window with only survival biasing and nothing else, the transmitted leakage is $8.26 \times 10^{-9} \pm 9.3\%$ with 6.3 for a figure of merit. The lower weight bound in the source cell was chosen to be 50% lower than the particles' source weight. The lower weight bound for the rest of the cells was chosen to be a factor $\alpha$ less than the previous cell's lower weight bound where $\alpha$ for cell i was chosen as

$$(\text{starting weight})\alpha^i = \begin{array}{l}\text{transmission obtained} \\ \text{by previous short run.}\end{array} \qquad (7)$$

The upper weight bound was chosen to be five times the lower weight bound.

Using the exponential transform with survival biasing, no weight-cutoff game, and a transform-biasing parameter of 0.7, only a very short run was required to see a poor performance. The figure of merit was 1.5, and the transmitted leakage was $4.86 \times 10^{-8} \pm 39\%$ which is too high by a factor of six - in other words, completely unreliable.

Adding to the exponential transformation a weight-cutoff game (but not the weight window) that is dependent on cell importances had the result that after 4.6 minutes of computer time the transmitted leakage was

$5.22 \times 10^{-9} \pm 19.2\%$ with a figure of merit of 4.2; after 10 minutes, $8.22 \times 10^{-9} \pm 26.7\%$; and after 17.6 minutes the leakage was $8.06 \times 10^{-9} \pm 18.4$ with 1.7 as the figure of merit. This example demonstrates the value in watching the behavior of a sample mean and its variance during the progress of a calculation. If either is unstable, the sample mean is unreliable. By not watching this behavior, a result (such as the leakage of $5.22 \times 10^{-9}$) may be incorrectly accepted as satisfactory based on an apparently low variance.

Applying the weight window and exponential transformation together produced the best of all results with a figure of merit of 22.6 and a transmitted leakage of $8.49 \times 10^{-9} \pm 3.0\%$.

The multigroup code MCMG using 30 groups and geometry splitting determined in the same manner as for MCNP was used on this problem. The figure of merit was 11.9, but the transmitted leakage was $2.17 \times 10^{-9} \pm 5.6\%$ which is low by a factor of four. Both the continuous-scattering angle and MORSE discrete-scattering angle treatments were used. No difference between the two was observed. For optically thin transmissions, however, the continuous treatment is superior.

MCNP itself can be used in a pseudo-multigroup fashion by using our discrete reaction cross-section set DRXS. These cross sections are equivalent to the regular continuous-energy cross sections used by MCNP except that the reaction cross sections have been collapsed into 240 energy groups. Using MCNP and these discrete cross sections along with geometry splitting on this problem, the transmitted leakage is $5.08 \times 10^{-9} \pm 6.8\%$ with 8.0 for the figure of merit.

All of these results are summarized in Table 4.

To our surprise, the performance of the weight window may be relatively insensitive to the size of the window. This problem was tried with the ratio of the upper to lower bound set at 400 to compare with the ratio of 5 used throughout this paper. The factor of 400 is consistent with a similar scheme used in MORSE. The results were virtually unchanged; the figure of merit was 19.5 and the leakage was $7.89 \times 10^{-9} \pm 10.6\%$. This implies that it is a very few tracks with very large weights that cause tallying problems. The problems caused by a weight dispersion have long been recognized, but the true nature of the dispersion may not have been fully appreciated.

The dramatic improvement in the performance of the exponential transform when it is used in conjunction with splitting at an upper weight limit seems to indicate that a substantial fraction of the tally variance is associated with very high-weight particles. Particles can accumulate a high weight by traveling against the transform vector for part of their trajectory. With splitting at the upper weight limit, the distribution of tally scores per source particle for each high-weight particle is shifted from a binary distribution of scoring or not scoring in one lump to a superposition of binary distributions with smaller components. The net

result is to reduce the variance while leaving the tally mean unchanged. The computational time involved is relatively small because the high-weight particles are relatively infrequent, and so a net gain is achieved in the figure of merit.

The biggest surprise we had in doing the calculations for this paper was the disagreement between the continuous-energy and multigroup results. We see from Table 4 that the MCMG multigroup results underpredict the continuous-energy results by a factor of almost 4. The group cross sections consist of 30 neutron groups from the ENDF/B-IV evaluation with a weighting spectrum which is a fission spectrum matching a 1/E spectrum for the energy range of interest.[9] In Table 5 we compare the partial leakage $J^+$ in the direction of penetration at 15-cm intervals through the concrete for continuous-energy and multigroup-collision treatments. It can be seen that the discrepancy appears to grow systematically. The column labeled "DRXS" is a calculation with the 240-group discrete-reaction cross sections using MCNP. The results of the DRXS calculations fall in between the continuous-energy and the 30-group MCMG results. One may conclude that an energy self-shielding effect introduces a discrepancy into the multigroup results and that the magnitude of the discrepancy may be quite significant for deep-penetration applications using standard cross-section sets. Although this effect has been reported in transport through pure materials (most notably in thick iron shields), it might not be expected in mixtures such as concrete with significant masking of cross-section windows and the presence of hydrogen to lessen the importance of windows.

Table 4. Summary of Results for 100-cm-Radius by 200-cm-Thick Concrete Cylinder

| Method | Transmitted Leakage | % Error | FOM | Computer Minutes |
|---|---|---|---|---|
| MCNP, splitting | $8.21 \times 10^{-9}$ | 4.4 | 6.7 | 77 |
| MCNP, weight window | $8.26 \times 10^{-9}$ | 9.3 | 6.3 | 18.4 |
| MCNP, exponential transformation | $4.86 \times 10^{-8}$ | 39 | 1.5 | 4.4 |
| MCNP, exponential transformation and weight cutoff | $8.06 \times 10^{-9}$ | 18 | 1.7 | 17.6 |
| MCNP, exponential transformation and weight window | $8.49 \times 10^{-9}$ | 3.0 | 22.6 | 49.2 |
| MCMG, splitting | $2.17 \times 10^{-9}$ | 5.6 | 11.9 | 26.8 |
| MCNP, discrete reactions, splitting | $5.08 \times 10^{-9}$ | 6.8 | 8.0 | 27.0 |

Given the discrepancy between continuous-energy and multigroup Monte Carlo, an obvious question becomes what is the result of an $S_n$ calculation. Therefore, we made an $S_n$ calculation with the one-dimensional $S_n$ code ONETRAN.[10] The geometry was assumed to be a 200-cm Portland concrete slab of infinite lateral extent. An infinite extent is a very good approximation since the Monte Carlo calculations indicated the transverse leakage to be about $2 \times 10^{-5}$. Using the truncated fission spectrum (i.e., source energies greater than 3.68 MeV) and the same 30 group ENDF/B-IV cross-section set as used with MCMG, good convergence was achieved with ONETRAN using $\Delta r$ of 1.66 cm and an S-8 Lobatto quadrature; the leakage was $2.45 \times 10^{-9}$. Using the full fission spectrum source, the leakage was $2.71 \times 10^{-9}$. Good convergence with a Gauss quadrature was not achieved until an S-16 or greater quadrature was used. There are a couple of conclusions: (1) $S_n$ agrees with the MCMG result of $2.17 \times 10^{-9} \pm 5.6\%$ within two standard deviations, and (2) $S_n$ requires a Lobatto or high-order Gauss quadrature for good convergence in deep-penetration problems.

To verify that the transverse leakage was truly negligible and that the one-dimensional $S_n$ and MCMG results were comparable, an MCMG calculation was performed with infinite radial extent for the 200-cm-long concrete cylinder. The results were essentially identical to those with the 100-cm radius.

To further complete the picture (but not belabor the point), ONETRAN was also used with a 30-group ENDF/B-V multigroup cross-section set. The transmitted leakage was virtually identical with the ENDF/B-IV results from ONETRAN and MCMG. Finally, MCNP calculations were made with modified 240-group discrete-reaction cross sections based on ENDF/B-V. The cross sections for both silicon and oxygen were modified to accurately represent the large window in the total cross section for each nuclide, at 0.145 MeV for silicon and 2.35 MeV for oxygen. The result was the same as with the regular discrete cross sections in which the windows are averaged out. This indicates the difference between continuous energy and multigroup treatments is due to a self-shielding effect.

Another potential method to improve the results at the exit surface is to surround the surface with a DXTRAN sphere. DXTRAN, however, is generally only useful in situations where it is difficult to get tracks by a random walk to a particular place in the geometry in order to make a tally. This is not the case here since by geometric splitting an abundance of tracks gets to the surface tallies. In this case DXTRAN makes the problem more inefficient by adding additional arithmetic complexity for the computer to handle. However, if one is interested in calculating the flux at a point in the center of the exit surface, relatively few tracks are in the vicinity of any given point on the surface. A surface tally therefore is useless, and a point detector is required. Placing a DXTRAN sphere around a detector can improve the efficiency of a detector calculation significantly.

Table 5. Comparison of Partial Leakage as a Function of Method and Thickness

| Surface | $J^+$MCNP | $J^+$DRXS | $J^+$MCMG | MCNP/DRXS | MCNP/MCMG |
|---|---|---|---|---|---|
| 15 cm | 7.44E-2 (.68%) | 7.38E-2 (.62%) | 7.35E-2 (.46%) | 1.01 | 1.01 |
| 30 | 2.66E-2 (6.6%) | 2.58E-2 (1.0%) | 2.48E-2 (.74%) | 1.03 | 1.07 |
| 45 | 8.07E-3 (1.5%) | 7.65E-3 (1.4%) | 7.00E-3 (1.0%) | 1.05 | 1.15 |
| 60 | 2.26E-3 (1.9%) | 2.14E-3 (1.8%) | 1.79E-3 (1.3%) | 1.06 | 1.26 |
| 75 | 6.14E-4 (2.4%) | 5.69E-4 (2.2%) | 4.40E-4 (1.7%) | 1.08 | 1.40 |
| 90 | 1.61E-4 (2.9%) | 1.48E-4 (2.7%) | 1.06E-4 (2.1%) | 1.09 | 1.52 |
| 105 | 4.25E-5 (3.5%) | 3.81E-5 3.2%) | 2.55E-5 (2.5%) | 1.12 | 1.67 |
| 120 | 1.14E-5 (4.1%) | 9.62E-6 (3.7%) | 5.89E-6 (3.0%) | 1.19 | 1.94 |
| 135 | 3.09E-6 (4.7%) | 2.41E-6 (4.4%) | 1.40E-6 (3.4%) | 1.28 | 2.21 |
| 150 | 7.99E-7 (5.3%) | 6.18E-7 (5.0% | 3.31E-7 (3.9%) | 1.29 | 2.41 |
| 165 | 2.13E-7 (6.0%) | 1.59E-7 (5.7%) | 7.77E-8 (4.4%) | 1.34 | 2.74 |
| 180 | 5.63E-8 (6.8%) | 3.91E-8 (6.1%) | 1.81E-8 (4.9%) | 1.44 | 3.11 |
| 200 | 8.20E-9 (7.9%) | 5.08E-9 (6.8%) | 2.17E-9 (5.6%) | 1.61 | 3.78 |

## 20-cm-Radius Problem

This problem is identical to the 100-cm-radius problem in every aspect except for the radius. The smaller radius now makes the transverse and backscattered leakages almost identical, $3.84 \times 10^{-2} \pm 0.4\%$. This problem

runs only slightly less efficiently than the 100-cm-radius problem. The reason is that although it is harder to get particles through the cylinder, less time is spent on particles wandering around radially. They are killed by escaping.

This problem was done in only two modes: splitting with MCNP and MCNP with a combination of the weight window and exponential transformation. The exponential transformation by itself on this problem performs very poorly. The importances for splitting were set using the same technique as before, and another (but different) combination of two-for-one and four-for-one splitting resulted. The importance in the last cell was 21233664 as compared to 4194304 for the 100-cm-radius problem. For the case of splitting, the transmitted leakage is $7.50 \times 10^{-10} \pm 5\%$ with 6.0 as a figure of merit. The weight window and transformation (biasing parameter is again 0.7) result is $8.17 \times 10^{-10} \pm 4.9\%$ with 21.5 as a figure of merit.

From the calculation with splitting, the transmitted neutron dose is $2.74 \times 10^{-17} \pm 7.0\%$ mrem/per neutron, and the transmitted flux is $8.06 \times 10^{-13} \pm 6.9\%$ neutron/$cm^2$.

DXTRAN is also inappropriate for this case as was for the 100-cm-radius case; the figure of merit is reduced by its use.

## BENT-PIPE PROBLEM

This problem is also divided into two parts, both of which are much less demanding than the previous 200-cm-concrete problem. In both cases a 20-cm-radius pipe that is 240-cm long along the axis has a 90° bend in the center and is jacketed concentrically by a 20-cm-thick region of ordinary Portland concrete. In the first case, the pipe is filled with liquid sodium, and in the second case the pipe is void. The geometry is shown in Figure 2. With the sodium, the attenuation from one end to the other is about $10^6$ and with the void about $10^3$.

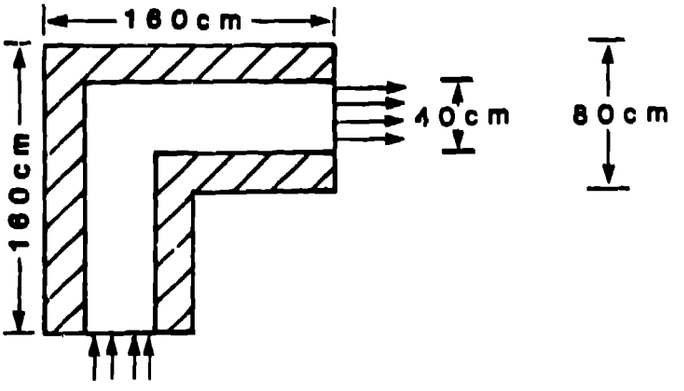


Figure 2. Bent Pipe Jacketed by Concrete.

The source for both cases is the same. It is an area source incident on one end of the pipe (but not including the jacket) with the energy and angular distribution given by

$$S(E,\mu) = \frac{\text{const.}}{E} \qquad \text{(1/E spectrum)} \tag{8}$$

$$= 0 \text{ otherwise} ,$$

where $\mu = +1$ is the cosine of the coaxial direction at the entrance plane. The procedure used to sample this distribution is given in the Appendix at the end of this paper. Constraints on the source are $8.32 \text{ eV} < E < 184 \text{ keV}$ and $0.8 < \mu < 1$.

The tally used to compare the various methods is the leakage transmitted out the opposite end of the pipe (pipe only and not including the jacket) within the direction $0.8 < \mu < 1.0$ where $\mu = +1$ is the cosine of the coaxial direction at the exit plane. Results of other tallies will be reported, however. The energy cutoff in all cases is 8.32 eV.

## Sodium-Pipe Problem

The sodium density used is $0.705 \text{ g/cm}^3$ which is appropriate for sodium temperatures of approximately 1000°C. This problem is representative of design features in fast breeder coolant loops and possibly in fusion reactor coolant loops.

With only survival-biasing and a weight-cutoff game, in two minutes of computer time, no tallies were made. In fact, out of 33878 source neutrons, only nine had made it around the 90° bend. No particle got within 40 cm of the pipe exit.

In this problem, the mean free path averaged over collisions for sodium is about 16 cm and about 2 cm in the concrete. Therefore, plane splitting surfaces were placed across the axis of the pipe at 20-cm intervals. A 45° plane was also added where the two legs of the pipe intersect. Radial splitting was used in this problem by adding two concentric cylinders within the concrete jacket to be used as splitting surfaces. The first cylindrical splitting surface was placed 2 cm inside the concrete jacket, and the second was placed outward in the radial direction another 2 cm.

To set the importances, two runs of half a minute each were made to level the track population in the pipe between the source plane and the tally plane. Relative to the corresponding axial importance in the pipe, the radial importances were decreased by a factor of two for each of the first two sleeves and then a factor of four for the outer sleeve. To show that this elaborate radial setup is really not necessary, another run was made with only one radial-splitting surface in the middle of the concrete jacket. The importances of the inner radial cells were reduced by

a factor of two and by another factor of four for the outer radial cells. The figure of merit was 62 with the two concentric splitting surfaces and 58 with only one in the center of the jacket. The two surfaces are more effective in killing outward-bound tracks and maximizing backscattered tracks, but the extra cells and surfaces required more computation time.

In applying the weight window to the sodium pipe, the lower weight bound was derived from the set of importances used in the run with splitting. The lower bound was taken to be $3/I_i$, where $I_i$ is the importance for cell i. The factor three was chosen so that the source particles would start within the weight window. The upper weight bound was taken to be five times the lower weight bound based on previous with the weight window, it was used with the biasing parameter p set to 0.4 in one case and to 0.7 in another.

A multigroup run was made with MCMG using geometry splitting with different axial-splitting planes and with one concentric splitting surface midway between the inner and outer surface of the concrete jacket.

Results of the above cases are summarized in Table 6.

Table 6. Results of Bent Sodium Pipe

| Method | Transmitted Leakage ($.8 < \mu < 1$) | % Error | FOM | Computer Minutes |
|---|---|---|---|---|
| MCNP, splitting | $5.83 \times 10^{-7}$ | 4.1 | 62 | 9.6 |
| MCNP, weight window | $6.38 \times 10^{-7}$ | 6.4 | 54 | 4.6 |
| MCNP, weight window, expo. trans.(.4) | $5.70 \times 10^{-7}$ | 5.7 | 67 | 4.6 |
| MCNP weight window, expo. trans.(.7) | $5.93 \times 10^{-7}$ | 6.3 | 55 | 4.6 |
| MCMG, splitting | $5.19 \times 10^{-7}$ | 5.0 | 46 | 8.7 |
| MCNP, splitting, DXTRAN | $5.92 \times 10^{-7}$ | 9.9 | 22 | 4.6 |

DXTRAN in conjunction with geometry splitting was tried for a couple of runs with MCNP. The DXTRAN sphere was placed around the sodium at the exit tally plane. A game was played with DXTRAN such that all contributions to the DXTRAN sphere were accepted within four mean free paths, and a Russian roulette game was played with contributions beyond four (a short run indicated about 90% of the contributions were being made within four mean free paths). In one case DXTRAN was tried with the setup with axial-splitting surfaces every 20 cm and with two concentric-splitting

surfaces in the concrete jacket; the figure of merit dropped from 62 to 22. Secondly, DXTRAN was tried with a very simple setup using one axial-splitting surface (four-for-one) at the 45° intersection of the cylinders and a second splitting surface (one-for-two) at the sodium-concrete interface; 0.7 was the figure of merit.

Results other than the transmitted leakage may be of interest. Using MCNP with geometry splitting, 56.5% of the starting weight was lost to energy cutoff, 0.3% to escape through the curved jacket, 0.9% to capture, and 41.2% to backscatter from the source plane. The transmitted leakage out of the sodium was $3.11 \times 10^{-7} \pm 4.3\%$ between 37° and 90° relative to the axis of the pipe at the exit and $5.83 \times 10^{-7} \pm 4.1\%$ between 0° and 37°. The leakage transmitted through the exit plane bounding the concrete jacket (an annular disk excluding the sodium in the center) was $6.27 \times 10^{-8} \pm 7.5\%$ between 37° and 90° and $5.05 \times 10^{-8} \pm 8.3\%$ between 0° and 37°. The neutron dose transmitted through the sodium exit plane was $1.28 \times 10^{-15} \pm 4.4\%$ mrem per neutron, and the dose transmitted through only the concrete at the exit plane was $6.39 \times 10^{-17} \pm 8.6\%$ mrem per neutron. The flux transmitted through the sodium exit plane was $1.01 \times 10^{-9} \pm 4.1\%$ neutrons/cm$^2$ and $5.02 \times 10^{-11} \pm 7.3\%$ neutrons/cm$^2$ through the concrete exit plane.

## Void-Pipe Problem

This problem is identical to the sodium-pipe problem except that the sodium is replaced by a void. Two surprises came from this problem: (1) intuition led to preliminary problems with geometry splitting, and (2) DXTRAN performed very impressively.

Trying this problem without any variance-reduction techniques, in two minutes of computer time 31449 neutrons started but only 358 got past the 90° bend, and 20 actually got to the exit tally plane.

The splitting surfaces were very similar to the sodium-pipe setup: axial planes every 20 cm and two interior concentric cylinders (one 4 cm into the concrete jacket from the void and the other another 4 cm into the jacket). The final axial importance before the exit was 4096 where it was 2519424 with the sodium. The attenuation from the source to the exit is on the order of $10^3$.

Initially the radial importances were set as with the sodium: relative to a given axial cell in the void, the first radial cell had an importance a factor of two less, the middle radial cell importance another factor of two less, and the outer radial cell a factor of four less than the middle cell. This setup led to a figure of merit of 16 which was surprising since the attentuation is three orders of magnitude less than with sodium where the figure of merit was 62.

Looking at the MCNP summary information, it was noted that each neutron created about 7 tracks, and each neutron had about 6.6 collisions. This says that on the average every time a track had a collision, it was

split. This was the clue to the problem: the importance of the inner sleeve of the concrete jacket was a factor of two less than the adjacent void region which meant that a track entering the concrete from the void underwent Russian roulette with 50% survival. If the track backscattered into the void, it was split two-for-one but then immediately went to the other side of the void where Russian roulette was played again, etc. Obviously this is very inefficient.

The next step was to set the importance of the inner sleeve equal to the importance of the adjacent void. The middle-sleeve importance was then reduced by a factor of two relative to the inner sleeve, and the outer-sleeve importance was reduced by a factor of four relative to the middle sleeve.

Playing other splitting games such as changing the thickness of the concrete sleeves and reducing the number of radial sleeves from three to two had relatively little effect.

The weight window by itself was used successfully in the problem; the exponential transformation is not applicable. The bounds of the windows were set based on experience and by experimenting with a couple of short runs and watching the behavior of the sample variance.

MCMG was used with geometry splitting incorporating one concentric splitting surface in the center of the concrete jacket. Furthermore, two scattering kernels were tried: (1) with a continuous-scattering angle and (2) with the MORSE discrete-scattering angle.

Results of these runs are summarized in Table 7.

Table 7. Results of Bent-Void Pipe

| Method | Transmitted Leakage ($.8 < \mu < 1$) | % Error | FOM | Computer Minutes |
|---|---|---|---|---|
| MCNP, splitting | $1.08 \times 10^{-3}$ | 5.6 | 33 | 9.6 |
| MCNP, weight window | $1.10 \times 10^{-3}$ | 4.2 | 53 | 10.7 |
| MCMG, splitting, cont. angle | $1.11 \times 10^{-3}$ | 3.7 | 60 | 12.2 |
| MCMG, splitting, discrete angle | $1.07 \times 10^{-3}$ | 3.8 | 57 | 12.1 |

The MCNP-with-splitting figure of merit is less than the others by about a factor of two and less than the sodium-pipe figure of merit also by

a factor of two. The reason for both of these observations is unclear at this point. It can be argued that the void pipe should take longer than the sodium pipe because with the void all scores at the tally come from time-consuming backscattering. With the sodium, a large number of tracks can get to the tally plane without having to backscatter.

DXTRAN with MCNP was tried on this problem in four cases: (1) with the above splitting setup that gave the 33 figure of merit, (2) with the same geometrical setup (all the cells and surfaces set up for splitting) but with importances set to unity, (3) no splitting and all internal cells and surfaces removed that were required for the earlier splitting, and (4) all the extra cells and surfaces still removed but split two-for-one axially where the two legs of the geometry intersect at 45° and reduce the importance of the adjacent concrete jacket by a factor of two relative to the void. The impressive results are shown in Table 8. The weight window was not used for any of these calculations, and there is a potential for further DXTRAN improvements by using it. All runs were for 4.6 minutes of computer time. Russian roulette was played for all contributions to the DXTRAN sphere beyond four mean free paths. In all cases the radius of the outer sphere was 30 cm, and the radius of the inner sphere was 20 cm.

Table 8. DXTRAN Results

| Case | Transmitted Leakage ($.8 < \mu < 1$) | % Error | FOM |
|---|---|---|---|
| 1 splitting, complex geometry | $1.07 \times 10^{-3}$ | 3.8 | 148 |
| 2 no splitting, complex geometry | $1.06 \times 10^{-3}$ | 4.0 | 134 |
| 3 no splitting, simple geometry | $1.08 \times 10^{-3}$ | 3.3 | 135 |
| 4 mild splitting, simple geometry | $1.04 \times 10^{-3}$ | 3.0 | 243 |

Some conclusions may be drawn from these DXTRAN calculations. The improvement from case 2 to case 3 points out the obvious: more cells and surfaces require more arithmetic by the computer; they don't come free. Comparing case 1 and case 2 suggests that when you are already doing a pretty good job by one other technique, an additional technique adds little more and may even hurt (this was observed in the other problems). Comparing cases 3 and 4 suggests that there is usually profit in adding a little obvious help to the random walk. Cases 1 and 4 suggest that a very complex, elaborate setup may be overkill; not only does it take a person longer to set up and debug a complicated geometry, it takes the computer a long time to get through it too.

Other results associated with this bent-void pipe include about 1% of the starting weight lost to escape through the curved jacket, 8% lost to backscatter, about 92% lost to energy cutoff, and 0.4% lost to capture. The leakage transmitted from the void at the exit plane between 37° and 90° is $1.65 \times 10^{-4} \pm 5.7\%$, the leakage transmitted from the concrete at the exit plane between 0° and 37° is $7.67 \times 10^{-5} \pm 12\%$ and $5.46 \times 10^{-5} \pm 7.7\%$ between 37° and 90°. The neutron dose through the void at the exit is $1.65 \times 10^{-12} \pm 5.8\%$ mrem per neutron and $6.64 \times 10^{-14} \pm 9.0\%$ through the concrete. The flux through the void at the exit is $1.16 \times 10^{-6} \pm 4.7\%$ neutrons/cm$^2$ and $5.25 \times 10^{-8} \pm 8.4\%$ neutrons/cm$^2$ through the concrete.

## CONCLUSIONS

It is virtually impossible to be able to say when to use one variance-reduction technique or another. One needs to have many techniques at his disposal. Furthermore, it is also virtually impossible to be able to prescribe how to use a particular technique. Experience in these matters has no substitute.

Despite the above disclaimer, we will attempt some general conclusions.

It appears the weight-window concept has merit when used in conjunction with other techniques that produce a large weight dispersion. It keeps from wasting time on low-weighted particles and keeps a tally and its variance from being overpowered by a few large-weighted scores. However, we at Los Alamos have not had enough experience with this tool to put it into MCNP permanently. We know relatively little about how to set the bounds of the window - especially if energy dependence is required.

The exponential transformation has very limited use by itself. It should not be used alone but in conjunction with something like the weight window. The performance and especially the reliability of the transformation are sensitive to the biasing parameter which, in our opinion, makes this technique dangerous to use except for the experienced Monte Carlo practitioner. We sometimes refer to the exponential transformation as the "dial-an-answer" technique, because the result of a calculation frequently appears to be a function of the biasing parameter.

Geometry splitting with Russian roulette is our most frequently-used technique. Although other schemes may buy more in particular situations, geometry splitting will virtually always give good returns. Furthermore, it is easy to understand and reliable. An important aspect that is apparent from the calculations in this paper is that performance is fairly insensitive within a broad range to how the splitting is implemented (two-for-one, four-for-one, where the surfaces are located, etc.)

Furthermore, it is not just enough to look at a figure of merit and a final sample error. You must also look at the sample mean and its error at

frequent intervals to make sure they have settled down and converged on a reliable result. In other words, look at the variance of the variance. For example, after a relatively few histories, a point-detector flux may have an indicated error of 10% but be in actual error by several factors. After a few more histories, both the flux and its error could be perturbed significantly. This procedure was not emphasized earlier in the paper, but it was used. It is simply wise practice - because it may give the only clue of an unreliable result.

Group X-6 is experimenting with analytically calculating the variance of the variance (or error of the error) and most of the MCNP calculations for this paper were done with a modification to MCNP for this purpose.[11] We recognize that there is very little quantitative information in the fourth moment, but qualitatively it appears that whenever the error of the error is of the same order as the error (both about 5 or 10%, for example) then the sample mean is reliable. But if the error is about 10% and the error of the error is 60%, the mean is unreliable.

One valid rule of thumb is to always make a few short, experimental runs to get a feel for the problem and to see the effect for different techniques and parameters. The code you are using should automatically provide you with enough basic information to allow you to evaluate and understand the run and its attributes. It has been our observation that the more experience a person has, the more reliance is put on preliminary runs. The less experience a person has, the more likely a job will be set up as quickly as possible, a long run attempted, and whatever comes out believed.

Finally, this paper has probably generated more questions than it has answered - especially in the area of multigroup calculations. Also, as applications become increasingly more complicated, there are other important and interesting topics such as the effect of representing a complex three-dimensional geometry by a lower-dimensional model. We look forward to addressing these and other questions in the future.

Acknowledgement

We wish to acknowledge P.D. Soran of X-6 for the ONETRAN calculation using ENDF/B-V data and for modifying the silicon and oxygen data in the discrete-reaction cross-section set.

## REFERENCES


1. "Neutron and Gamma-Ray Flux-to-Dose Rate Factors," ANSI/ANS-6.1.1-1977 (N666), American Nuclear Standards Neutron and Gamma-Ray Flux-to-Dose-Rate Factors, Am. Nuc. Soc. (Illinois, 1977).

2. LASL Group X-6, "MCNP - A General Monte Carlo Code for Neutron and Photon Transport," LA-7396-M, Revised (November, 1979).

3. O. L. Deutsch, "MCMG User's Guide," Internal X-6 Document (March, 1979).

4. L. L. Carter and C. A. Forest, "Transfer Matrix Treatments for Multigroup Monte Carlo Calculations - The Elimination of Ray Effects," Nuclear Science and Engineering, 59, 27 (1976).

5. N. M. Schaeffer, Editor, "Reactor Shielding for Nuclear Engineers," Published by U.S. A.E.C. Office of Information Services, p.451 (1973).

6. "The Analysis and Design of Concrete Radiation Shielding for Nuclear Power Plants," ANSI/ANS-6.4-1977 (N403), American Nuclear Standards Guidelines on the Nuclear Analysis and Design of Concrete Radiation Shielding for Nuclear Power Plants, Am. Nuc. Soc. (Illinois, 1977).

7. G. P. Estes and J. S. Hendricks, "Integral Testing of Some ENDF/B-V Cross Sections," Transactions of the ANS, 33, 679 (November, 1979).

8. R. E. MacFarlane, "Energy Balance of ENDF/B-V," Transactions of the ANS, 33, 681 (November, 1979).

9. R. J. Barrett and R. E. MacFarlane, "Coupled Neutron and Photon Cross Sections for Transport Calculations," LA-7808-MS (April, 1979).

10. T. R. Hill, "ONETRAN, A Discrete Ordinates Finite Element Code for the Solution of the One-Dimensional Multigroup Transport Equation," LA-5990-MS (June 1975).

11. G.P. Estes and E.D. Cashwell, "MCNP Variance Error Estimator," X-6 Activity Report, LA-8232-PR, p. 19 (July-December, 1979).

## Appendix

1. Fission-Spectrum Groups for MCMG

The source fraction per group, $S_g$, is determined from

$$S_g = \int_{E_{g+1}}^{E_g} \left(\frac{2}{\sqrt{\pi}T}\right)\sqrt{\frac{E}{T}}\, e^{-E/T}\, dE, \quad T = 1.30 \text{ MeV} \quad .$$

| Group | Lower Bound, MeV | $S_g$ |
|---|---|---|
| 1 | 15.0 | 3.0380E-5 |
| 2 | 13.5 | 7.8639E-5 |
| 3 | 12.0 | 2.3568E-4 |
| 4 | 10.5 | 1.1626E-3 |
| 5 | 7.79 | 5.9203E-3 |
| 6 | 6.07 | 1.7678E-2 |
| 7 | 3.68 | 1.0418E-1 |
| 8 | 2.865 | 9.1383E-2 |
| 9 | 2.232 | 1.0877E-1 |
| 10 | 1.738 | 1.1525E-1 |
| 11 | 1.353 | 1.1097E-1 |
| 12 | 0.823 | 1.8153E-1 |
| 13 | 0.50 | 1.1963E-1 |
| 14 | 0.303 | 6.9450E-2 |
| 15 | 0.184 | 3.6918E-2 |
| 16 | 0.0676 | 2.8169E-2 |
| 17 | 0.0248 | 6.6880E-3 |
| 18 | 0.00912 | 1.5188E-3 |
| | | 0.99955 |

2. Sample Energy E from Fission Spectrum

$$f(E) = \frac{2}{\sqrt{\pi}\,T}\sqrt{\frac{E}{T}}\, e^{-E/T}$$

$$T = 1.30 \text{ MeV}$$
$$E = 3T/2 = 1.95 \text{ MeV}$$

Let $\xi$ be a random number (0,1),

$$a = (-\ln \xi_0)\cos^2\left(\frac{\pi}{2}\,\xi_1\right) \text{ and}$$
$$E = T(-\ln \xi_3 + a) \quad .$$

3. Sample 1/E Energy Distribution, Angular Distribution, and Spatial Distribution

Let $\xi$ be a random number (0,1),

(a) Energy: $f(E) = (.10)/E$ $\quad 8.32 \text{ eV} < E < 184 \text{ keV}$

$$E = 0.184e^{-10\xi}$$

(b) Angular: $f(\mu) = \text{const.}$ $\quad 0.8 < \mu < 1$

$= 0$ $\quad$ otherwise

$$\mu = 0.8 + 0.2\xi$$

$\mu = +1$ is along y-axis

The direction cosines (u,v,w) = (0,1,0) must be rotated through the polar angle $\cos^{-1}\mu$ and through an azimuthal angle sampled uniformly from $(0,2\pi)$.

(c) Spatial: $y = 0$

$$x^2 + z^2 < 20^2 \quad .$$